Generation of time-bin-entangled photons without temporal postselection

Alessandro Rossi,* Giuseppe Vallone,* Francesco De Martini,* and Paolo Mataloni*
Dipartimento di Fisica della "Sapienza," Università di Roma, Roma, 00185 Italy
and Consorzio Nazionale Interuniversitario per le Scienze Fisiche della Materia, Roma, 00185 Italy
(Received 12 May 2008; published 23 July 2008)

We report on the implementation of an interferometric scheme that allows the generation of photon pairs entangled in the time-energy degree of freedom. This scheme does not require any kind of temporal postselection on the generated pairs and can be used even with lasers with short coherence time.

DOI: 10.1103/PhysRevA.78.012345 PACS number(s): 03.67.Bg, 42.50.Dv, 42.65.Lm

I. INTRODUCTION

Quantum entanglement represents the key ingredient of many quantum-information processes. It represents a unique resource that, associated with nonclassical correlations among separated quantum systems, can be used to perform computational [1,2] and cryptographic [3] tasks that are impossible with classical systems. An entangled state shared by two or more separated parties is a valuable resource for fundamental quantum communication protocols, such as quantum teleportation [4,5].

In quantum optics, entanglement based on discrete variables is created by the spontaneous parametric down conversion (SPDC) process in a nonlinear (NL) optical crystal under excitation of a laser beam, either in continuous wave (cw) or pulse operation. By this process highly pure entangled states are produced by encoding qubits in a particular degree of freedom (DOF) of the photons, such as polarization [6], linear and angular momentum [7–9], and energy-time [10]. More recently, the possibility of spanning a large Hilbert space by encoding two photons in more than one DOF at the same time was demonstrated by exploiting the so-called hyperentanglement [11–14]. Energy-time entanglement, also including the time-bin approach, generally realized with fiber interferometers [15], is based on the interferometric scheme proposed by Franson [10] which allows the creation of a superposition state of emission times. Relevant realizations of bulk schemes of this idea were also demonstrated [16,17].

In this paper we present a bulk scheme which allows the efficient creation of time-energy entanglement with SPDC photon pairs emitted by a type I phase-matched NL crystal. At variance with Franson's scheme, instead of two phase-locked interferometers (one for each photon), this apparatus is based on a single Michelson interferometer (MI) into which the two photons, traveling along parallel directions, are injected. This configuration reduces the problems of phase instability. Furthermore, by swapping the photon modes in one of the two MI arms (either the short or the long arm), the entangled state is automatically generated without any need of temporal postselection. In fact if one photon follows the short path and the other photon follows the long path, they will end on the same detector, thus giving no contribution to the coincidence counts. Furthermore, this scheme allows time-energy entanglement to be created with any kind of lasers that also have a very short coherence time.

The paper is organized as follows. Section II reviews Franson's unbalanced interferometer and the conditions that must be satisfied in order to observe time-bin entanglement. In Sec. III we describe the MI adopted in our experiment and the generation of the entangled state. Section IV describes the results of our experiment. Finally, in Sec. V we give the conclusions and indicate some possible use of such a scheme.

II. REVIEW OF FRANSON'S INTERFEROMETRIC SCHEME

Let us consider two photons, A and B, emitted by a SPDC source toward two different directions. Each one is injected into a Mach-Zehnder (MZ) interferometer (cf. Fig. 1).

Single photon interference arises if the imbalances between the MZ's long and the short arms

$$\Delta x_i = \ell_i - s_i, \quad i = A,B \tag{1}$$

do not exceed the single photon coherence length, $c\tau_c$. We can model Franson's scheme as given by two independent sequential operations, corresponding, respectively, to a preparation and a measurement device (see Fig. 1). The first

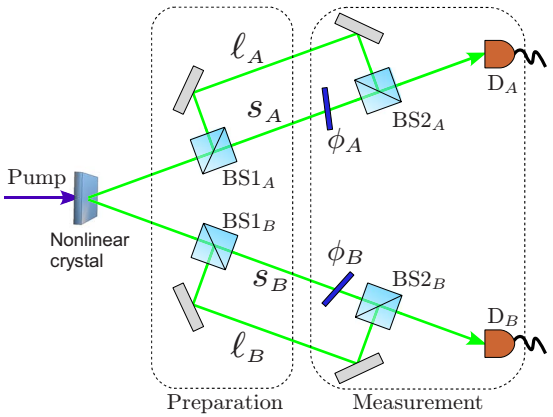

FIG. 1. (Color online) Scheme of Franson's interferometer. The long and short arms are labeled as ℓ and s, respectively. The thin glasses (ϕ_A, ϕ_B) can be used to change the phase in the measurement.

*http://quantumoptics.phys.uniroma1.it/

one is realized by the first pair of beam splitters ($BS1_i$) and generates the state

$$|\Psi_0\rangle = \frac{1}{2}(|s_A\rangle + |\ell_A\rangle)(|s_B\rangle + |\ell_B\rangle). \quad (2)$$

The detection occurring after the second pair of beam splitters, $BS2_i$, projects $|\Psi_0\rangle$ into the state

$$|\Phi_0\rangle = \frac{1}{2}(|s_A\rangle + e^{i\phi_A}|\ell_A\rangle)(|s_B\rangle + e^{i\phi_B}|\ell_B\rangle). \quad (3)$$

The single counts oscillate as $\cos^2\frac{\phi_i}{2}$ because of single photon interference and the coincidence rate is expressed as

$$C(\phi) = C_0 \cos^2\frac{\phi_A}{2}\cos^2\frac{\phi_B}{2}. \quad (4)$$

In order to create time-bin entanglement the following conditions must be fulfilled when operating under cw pumping (we consider the two imbalances $\Delta x_A = \Delta x_B \equiv \Delta x$ equal).

(i) The arm length difference must be long compared to the coherence length of photon wave packets:

$$\Delta x > c\tau_c. \quad (5)$$

This condition avoids single photon interference and, by working with photons in the visible range (400–700 nm) detected within a bandwidth of few nanometers, it is typically satisfied with an imbalance $\Delta x \geq 100\ \mu$m.

(ii) The imbalance Δx must be shorter than the pump coherence length τ_{pump}:

$$\Delta x < c\tau_{\text{pump}}. \quad (6)$$

This condition guarantees the coherent superposition of the $|s_A,s_B\rangle$ and $|\ell_A,\ell_B\rangle$ events.

(iii) Δx must be long enough to discard by postselection the events occurring when one photon takes the short path and the other takes the long path and vice versa. These measurement outcomes correspond to the events $|s_A,\ell_B\rangle$ and $|\ell_A,s_B\rangle$. This latter requirement imposes the condition

$$\Delta x > c\Delta T_c, \quad (7)$$

where ΔT_c represents the duration of the coincidence window. This condition imposes a strong constraint on the imbalance Δx.

Once the above conditions are satisfied, the events $|s_A,\ell_B\rangle$ and $|\ell_A,s_B\rangle$ are distinguishable and may be discarded by a suitable choice of the time coincidence window, while $|\ell_A,\ell_B\rangle$ and $|s_A,s_B\rangle$ are indistinguishable and generate the interference. Indeed, it is impossible to determine if the photons are emitted at time t_0 and both travel through the long paths or are emitted at time $t_0+\Delta x/c$ and both travel through the short paths. In this configuration, the first beam splitters ($BS1_A$ and $BS1_B$) generate the state

$$|\Psi\rangle = \frac{1}{2}|\psi\rangle\langle\psi| + \frac{1}{4}(|s_A,\ell_B\rangle\langle s_A,\ell_B| + |\ell_A,s_B\rangle\langle\ell_A,s_B|), \quad (8)$$

where

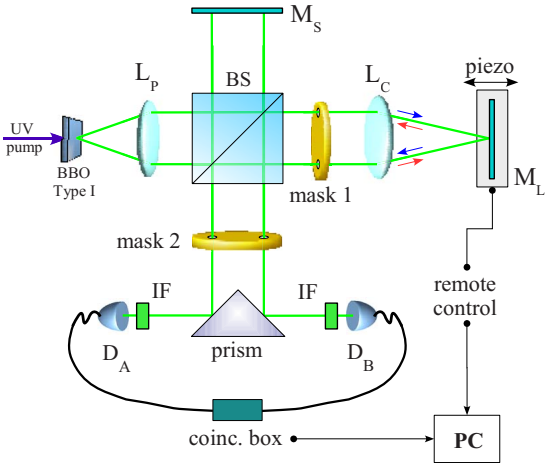

FIG. 2. (Color online) Michelson interferometric scheme used to generate time-bin entanglement.

$$|\psi\rangle = \frac{1}{\sqrt{2}}(|s_A,s_B\rangle + |\ell_A,\ell_B\rangle). \quad (9)$$

The second beam splitters ($BS2_i$), together with the subsequent detection, perform the projection into the entangled state

$$|\Phi\rangle = \frac{1}{\sqrt{2}}(|s_A,s_B\rangle + e^{i(\phi_A+\phi_B)}|\ell_A,\ell_B\rangle) \quad (10)$$

with phase shifts ϕ_i realized by using two thin glass plates.

From Eqs. (6) and (7) it follows that the coherence time τ_{pump} of the pump beam must exceed the coincidence window

$$\tau_{\text{pump}} > \Delta T_c. \quad (11)$$

Typically, the minimum achievable duration of the coincidence window is 1.5 ns, hence efficient postselection can be obtained if $\Delta x \geq 60$ cm. This generally imposes the use of a single longitudinal mode laser in order to satisfy conditions (i)–(iii) in the cw regime. When operating with an unbalanced bulk interferometer, any length variation of the corresponding arms affects the stability of the entangled state, hence this configuration requires a critical stabilization of the phase. In the case of an unbalanced interferometer based on single mode fibers, the phase is kept stable by temperature stabilization of the fibers.

III. EXPERIMENT

In the experimental apparatus (see Fig. 2) SPDC photon pairs are generated at degenerate wavelength (wl) $\lambda = 532$ nm by a 1 mm slab of β-barium borate (BBO), cut for type I phase matching, excited by a cw single longitudinal mode laser (MBD-266, Coherent, coherence time $\tau_{\text{pump}} > 0.1\ \mu$s, $\lambda_{\text{pump}} = 266$ nm).

In order to inject the two photons into a single MI, the corresponding **k** modes must be parallel. On this purpose, the characteristic SPDC conical emission of the NL crystal is transformed into a cylindrical one by a spherical lens (L_P)

whose relative distance from the BBO corresponds exactly to its focal length $f_L=9.5$ cm. The lens position is carefully set by optimizing the visibility of the single photon interference. The two photons, traveling along parallel directions, are injected into the input port of the MI shown in Fig. 2. In this setup the same BS is used both for the preparation of the state in the first passage of the photons (corresponding to the BS1s in Franson's scheme) and for the final measurement in the second passage (equivalent to the BS2s).

The photons' directions are carefully selected by two 2-hole masks (mask 1 and 2 in Fig. 2), the first inserted in the long arm and the second one at the MI output. Photons can travel along the short or long path, after the partition from a symmetric ($R=T=0.50\pm0.03$) beam splitter (BS). After reflection by mirrors M_s and M_ℓ, each photon experiences a new BS reflection-transmission process with relative path delay $\Delta x_0=2(\ell-s)$ [21]. The BS output beams are then directed by a reflecting prism toward two single photon counting (SPCM-AQR 14) modules and detected within a bandwidth $\Delta\lambda=4.5$ nm, which corresponds to a single photon coherence time of $\tau_c\sim100$ fs. The relative phase of path contributions $|s_A,s_B\rangle$ and $|\ell_A,\ell_B\rangle$, namely $\phi_A+\phi_B$ of Eq. (10), can be modified by a piezo transducer that finely changes the position of mirror M_ℓ on the ℓ arm. The simultaneous action of the piezo transducer on both photons in the long path determines the same change on ϕ_A and ϕ_B. This single MI configuration allows the phase instability problems to be minimized, as said.

The key element of our setup is represented by the swapping operation between the two photons, performed in the ℓ arm of MI. It is realized by the lens L_C (see Fig. 2), aligned in such a way that mirror M_L is located exactly in the focal plane of L_C. By this configuration we can only detect coincidences if both photons travel along the same arm of the MI. In fact if, for instance, the first photon goes through the ℓ path and the second follows the s path (i.e., if we consider the event $|\ell_A,s_B\rangle$, after the second BS passage they will end on the same detector. Thus no coincidence is detected in this case. The same happens for the $|s_A,\ell_B\rangle$ event.

By this setup it is no longer necessary to perform temporal postselection to discard the events $|\ell_A,s_B\rangle$ and $|s_A,\ell_B\rangle$. They are simply rejected by the coincidence measurement. In this way the conditions (i) and (iii) are not required anymore. The first one is not necessary because single photon interference cannot occur in this configuration. On the other hand, the condition (iii) is not necessary because the events $|\ell_A,s_B\rangle$ and $|s_A,\ell_B\rangle$ are not discarded by the arrival time, but because of the arrival position. This scheme thus allows time-entanglement also with a very short coherence time of the pump. Indeed time-entanglement is present also if the condition (11) is not satisfied. Moreover, the difference Δx can be very small.

IV. EXPERIMENTAL RESULTS

Before describing the experimental results, we show the interference pattern obtained in the condition of best L_P alignment. We used the same setup of Fig. 2 with some little modifications on the long arm: precisely, we set its length equal to the short arm and removed the swapping lens L_C. In this way single photon interference determines a fringe pattern whose visibility is maximized when the two photons' directions are exactly parallel. This is obtained when the distance between L_P and the BBO crystal is equal to the lens focal length. The position of L_P is then carefully set by maximizing the interference. The corresponding results are shown in Fig. 3.

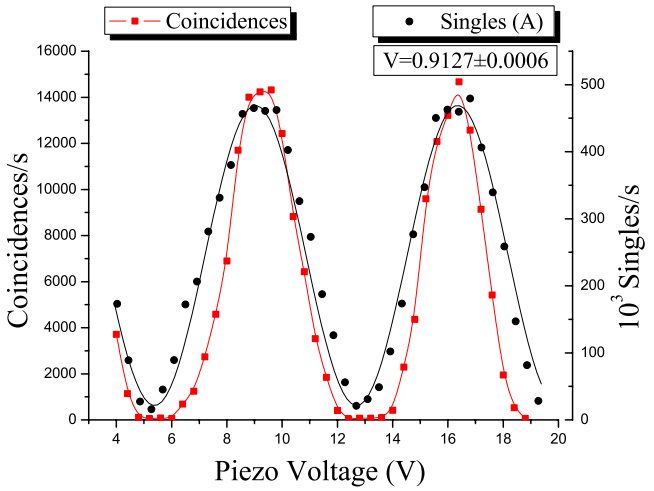

FIG. 3. (Color online) Single (right) and coincidence (left) counts measured by our apparatus in the presence of single photon interference. The high visibility of the single count oscillation is used to test the correct position of the lens L_P. Coincidence counts also oscillate in agreement with Eq. (4).

After optimization of lens L_P we set the measurement apparatus in the configuration of Fig. 2. Here the imbalance is $\Delta x_0=120$ cm and we do not expect any single count oscillation, while time-bin entanglement will arise. Figure 4 shows the coincidence rate as a function of the voltage applied to the piezo transducer for a coincidence window

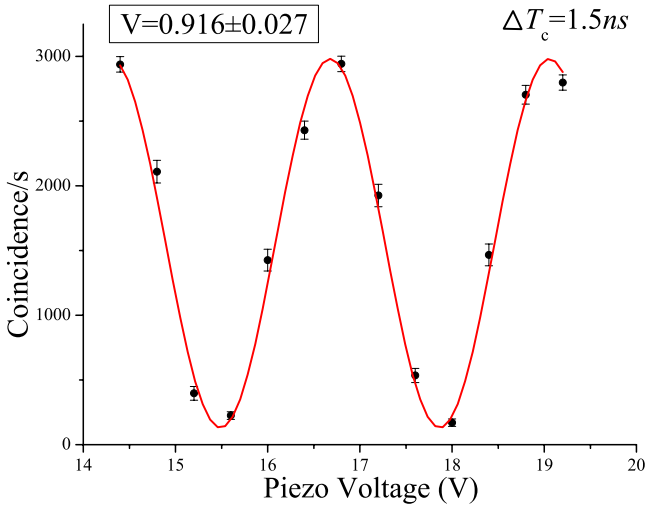

FIG. 4. (Color online) Coincidence counts after accidental coincidence subtraction with $\Delta T_c=1.5$ ns in the case of time-bin entanglement. Error bars are calculated by considering both the Poissonian statistic and the uncertainty of the voltage applied to the piezo transducer.

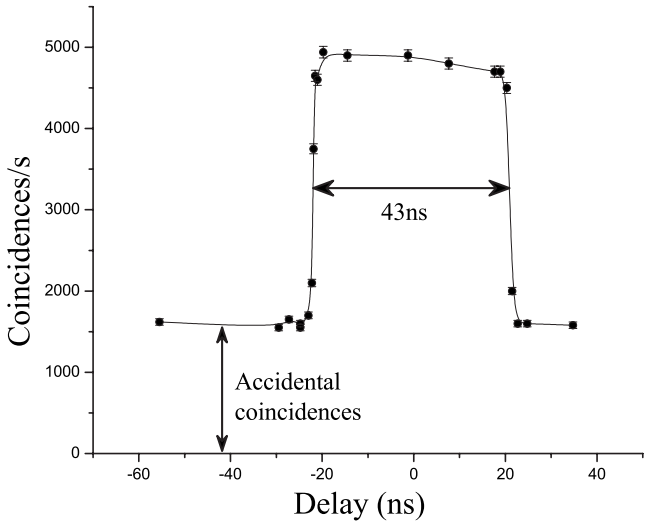

FIG. 5. Measurement of a coincidence window $\Delta T_c = 21.5$ ns. Fixing the arrival time of the first photon, we measured the coincidences by varying the arrival time delay of the second photon. The baseline (~1600 coinc/s) corresponds to the accidental coincidence contribution. This value is in agreement with that obtained by Eq. (13).

$\Delta T_c = 1.5$ ns. Each datum is obtained in 1 s acquisition time. As usual, the visibility is defined as

$$V = \frac{C_{\max} - C_{\min}}{C_{\max} + C_{\min}}, \tag{12}$$

where $C_{\max(\min)}$ is the maximum (minimum) coincidence value in the oscillation pattern. Equivalently, it is defined as the parameter V in the fitting function $C(x) = c_0\{1 + V\cos[\omega(x - x_0)]\}$, with x corresponding to the piezo transducer voltage. The high visibility value $V = 0.916 \pm 0.027$ clearly exceeds $\frac{1}{\sqrt{2}} \sim 0.71$ which is the upper limit for separable states [22] and demonstrates time-bin entanglement [15,16]. In fact if the events $|s_A, \ell_B\rangle$ and $|\ell_A, s_B\rangle$ were not discarded the visibility could not be larger than 0.5. It is worth noting that the small value of ΔT_c would allow these events to be discarded even in the case of a standard Franson's scheme.

Let us now describe the case of a much longer coincidence window, $\Delta T_c = 21.5$ ns. The value of ΔT_c was measured by observing the coincidence pattern as a function of the relative temporal delay between the two photons (see Fig. 5). Precisely, we fix the arrival time of the first photon and measure the coincidence number by varying the arrival time δt of the second photon. Since the coincidence box detects coincidences regardless of which photon comes first, we detect real coincidences if -21.5 ns $\leq \delta t \leq 21.5$ ns. In this condition, by using the standard Franson's scheme the imbalance Δx_0 would not allow time-bin entanglement because the condition (7) would be violated. In our scheme Eq. (7) is not necessary anymore; here we can generate time-bin entanglement even if the imbalance Δx_0 is shorter than the coincidence window ΔT_c. In Fig. 6 we show the coincidence pattern obtained with $\Delta T_c = 21.5$ ns. We report here the raw data, i.e., without any accidental coincidence subtraction. As

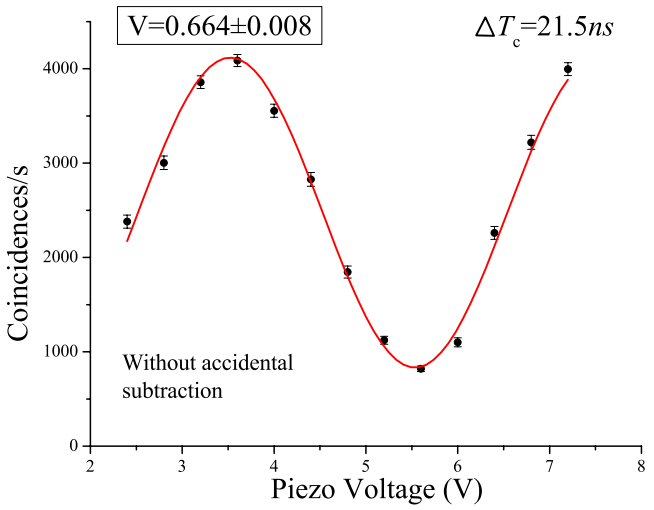

FIG. 6. (Color online) Raw coincidence counts (without accidental coincidence subtraction) with coincidence window $\Delta T_c = 21.5$ ns.

expected, even if the visibility is quite low $V = 0.664 \pm 0.008$, it is remarkable that this value is larger than the classical limit 0.5. In this condition the standard Franson's scheme would not allow a visibility >0.5, due to the impossibility of discarding the events $|s_A, \ell_B\rangle$ and $|\ell_A, s_B\rangle$. We also report in Fig. 7 the experimental results of Fig. 6 after accidental coincidence subtraction. These are estimated by using the expression

$$C_{acc} = 2S_A S_B \Delta T_c, \tag{13}$$

where S_A and S_B are the single counts measured at detectors D_A and D_B, respectively. The new visibility is now $V = 0.949 \pm 0.005$ which is comparable within the errors with that obtained with $\Delta T_c = 1.5$ ns.

V. CONCLUSIONS

In this paper we have described an interferometric scheme to create time-bin entanglement based on two photon states. It consists of a Michelson interferometer in which two de-

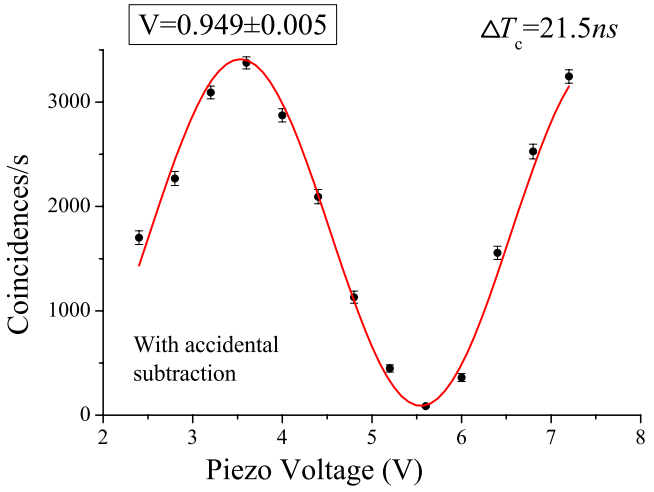

FIG. 7. (Color online) Coincidence counts with 21.5 ns coincidence window after accidental subtraction.

generate photons, created by spontaneous parametric down conversion in a type I phase matched NL crystal and traveling along parallel directions, are injected. Compared with the standard Franson's scheme, which adopts two different unbalanced interferometers and creates time-bin entanglement by temporal postselection, our scheme presents significant advantages.

(1) Since it is based on a common interferometer for the two photons, it avoids most of the problems related to phase instabilities.

(2) The scheme avoids the use of temporal postselection to generate the entanglement. Indeed, by using a simple lens in one of the interferometer arms, it operates under the spatial swapping of the two photon **k** modes.

(3) Under cw operation, this scheme can work with any kind of laser (even with a short coherence time) used to pump the parametric process.

The experimental results obtained by this scheme indicate that it represents a possible solution for several applications of quantum communication and quantum computation. In particular, it can be used to increase the dimension of a multi-degree-of-freedom two-photon state. For instance, it can be used to add two more qubits by time-energy entanglement to a four-qubit polarization-momentum hyperentangled state [18,19]. This would allow the realization of a more complex algorithm thanks to the enhanced number of qubits. Concerning communication, the time-bin entanglement can be used with other degrees of freedom to enhance the channel capacity in dense-coding protocols [20]. By referring to the parametric source sketched in Fig. 8, at the beginning, polarization entanglement is generated by double passage of the pump beam and of the photon pair through a type I BBO crystal, and a $\lambda/4$ wave plate after reflection from a spherical mirror M. Then, linear momentum entanglement is obtained by properly selecting (for instance, with a mask) four **k** modes of the SPDC conical emission of the type I crystal. In

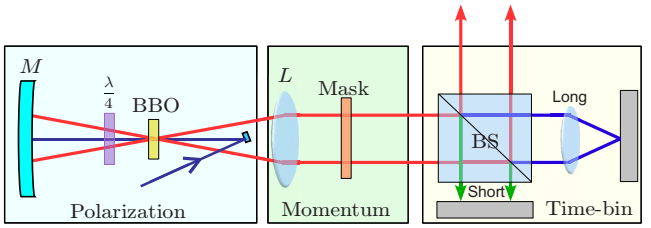

FIG. 8. (Color online) Scheme for the generation of two-photon polarization and momentum and time-bin entangled states.

this way polarization-momentum hyperentanglement is generated (see [12] for a detailed description of the hyperentangled source). This state corresponds to a two-photon four-qubit state. By injecting the four modes into the MI described in this paper we will add time-bin entanglement and allow each photon to encode three qubits in the different DOFs. This will generate the polarization and momentum and time-bin entanglement of two photons:

$$|\chi\rangle = \frac{1}{\sqrt{8}}(|H_A,H_B\rangle + |V_A,V_B\rangle) \otimes (|a_1,b_2\rangle + |a_2,b_1\rangle) \otimes (|s_A,s_B\rangle + |\ell_A,\ell_B\rangle), \tag{14}$$

where H, V are, respectively, the horizontal and vertical polarization, while a_1, a_2 (b_1, b_2) are the two modes (or linear momentum states) of the photon A (B). This experiment is at the moment under investigation.

ACKNOWLEDGMENTS

Thanks to Gaia Donati for the contribution given in realizing the experiment. This work was supported by the PRIN 2005 of MIUR (Ministero dell'Universià e della Ricerca), Italy.

[1] R. Raussendorf and H. J. Briegel, Phys. Rev. Lett. **86**, 5188 (2001).
[2] E. Knill, R. Laflamme, and G. J. Milburn, Nature (London) **409**, 46 (2001).
[3] A. K. Ekert, Phys. Rev. Lett. **67**, 661 (1991).
[4] D. Boschi, S. Branca, F. De Martini, L. Hardy, and S. Popescu, Phys. Rev. Lett. **80**, 1121 (1998).
[5] D. Bouwmeester, J.-W. Pan, K. Mattle, M. Eibl, H. Weinfurter, and A. Zeilinger, Nature (London) **390**, 575 (1997).
[6] P. G. Kwiat, K. Mattle, H. Weinfurter, A. Zeilinger, A. V. Sergienko, and Y. Shih, Phys. Rev. Lett. **75**, 4337 (1995).
[7] J. G. Rarity and P. R. Tapster, Phys. Rev. Lett. **64**, 2495 (1990).
[8] N. K. Langford, R. B. Dalton, M. D. Harvey, J. L. O'Brien, G. J. Pryde, A. Gilchrist, S. D. Bartlett, and A. G. White, Phys. Rev. Lett. **93**, 053601 (2004).
[9] A. Mair, A. Vaziri, G. Weihs, and A. Zeilinger, Nature (London) **412**, 313 (2001).
[10] J. D. Franson, Phys. Rev. Lett. **62**, 2205 (1989).
[11] C. Cinelli, M. Barbieri, R. Perris, P. Mataloni, and F. De Martini, Phys. Rev. Lett. **95**, 240405 (2005).
[12] M. Barbieri, C. Cinelli, P. Mataloni, and F. De Martini, Phys. Rev. A **72**, 052110 (2005).
[13] T. Yang, Q. Zhang, J. Zhang, J. Yin, Z. Zhao, M. Zukowski, Z.-B. Chen, and J.-W. Pan, Phys. Rev. Lett. **95**, 240406 (2005).
[14] J. T. Barreiro, N. K. Langford, N. A. Peters, and P. G. Kwiat, Phys. Rev. Lett. **95**, 260501 (2005).
[15] J. Brendel, N. Gisin, W. Tittel, and H. Zbinden, Phys. Rev. Lett. **82**, 2594 (1999).
[16] P. G. Kwiat, A. M. Steinberg, and R. Y. Chiao, Phys. Rev. A **47**, R2472 (1993).
[17] P. R. Tapster, J. G. Rarity, and P. C. M. Owens, Phys. Rev. Lett. **73**, 1923 (1994).
[18] G. Vallone, E. Pomarico, F. De Martini, and P. Mataloni, Phys. Rev. Lett. **100**, 160502 (2008).
[19] G. Vallone, E. Pomarico, F. De Martini, and P. Mataloni, Laser Phys. Lett. **5**, 398 (2008).

[20] J. T. Barreiro, T.-C. Wei, and P. G. Kwiat, Nature (London) **4**, 282 (2008).

[21] The factor 2 with respect to Franson's scheme is due to the double passage in each arm.

[22] Under some reasonable assumptions, if the coincidence counts vary sinusoidally as a function of $\phi_A+\phi_B$ with visibility larger than 0.71, time-bin entanglement is demonstrated (see Ref. [16]).